Cement and Concrete Research 41 (2011) 380–391

Contents lists available at ScienceDirect

Cement and Concrete Research

journal homepage: http://ees.elsevier.com/CEMCON/default.asp

Impact of time-dependant thermal expansion coefficient on the early-age volume changes in cement pastes

I. Maruyama *, A. Teramoto

Graduate School of Environmental Studies, Nagoya University, Faculty of Engineering, Building 3, No. 580, Furo-cho, Chikusa-ku, Nagoya 464-8603 Japan

ARTICLE INFO

Article history:
Received 8 September 2010
Accepted 11 January 2011

Keywords:
Fresh concrete
Shrinkage (C)
Cement paste
Granulated blast-furnace slag
Thermal expansion coefficient

ABSTRACT

Volume changes and time-dependent thermal expansion coefficient were determined at early stages and the measured total strain was separated into thermal strain and autogenous strain. Cement paste specimens were subjected to temperature histories that imitated hydration-induced temperature rise of the mass concrete. It was shown that the thermal expansion coefficient increased significantly with the development of hydration and became more conspicuous when the ground granulated blast furnace slag was added. The time-dependant increase of thermal expansion coefficient, due to self-desiccation, could result in considerable shrinkage strain at the end of the temperature history. The impact of the time-dependant increase of thermal expansion coefficient might be taken into account as one of the necessary factors in the crack control design from now and cannot even be neglected within the range of the water to binder ratio of this study, because the shrinkage originated in that effect sometimes exceed the autogenous shrinkage.

1. Introduction

When ground granulated blast furnace slag, GGBFS, is admixed with concrete, thermal expansion coefficient [1] and autogenous shrinkage [2] increase compared with those of normal concrete. The increase in the autogenous shrinkage is more significant when subjected to high temperature histories due to the hydration reactions. The Japanese guideline for the crack control of mass concrete specified that the ground granulated blastfurnace slag cement concrete should presume its thermal expansion coefficient 20% larger than that of the normal concrete and the designed autogenous shrinkage should be larger than that with the ordinary Portland cement—OPC [3]. The aim of this study includes the discussion on the volume change mechanism of the GGBFS-added concrete.

The autogenous shrinkage is generally determined by subtracting thermal dilatation out of the measured total strain with an assumption that the thermal expansion coefficient is constant throughout the measurement [4,5]. As far as the thermal crack risk is discussed in terms of the total strain, this may not invite significant problems while there still is a possibility of confusing the effects of thermal strain and autogenous shrinkage. In fact, countermeasures for the thermal cracking would become significantly different whether the emphasis is laid on the reduction of the autogenous shrinkage or control of the thermal dilatation.

In this study, careful examination of the factors affecting the thermal cracking was attempted and measurements of total strain and thermal expansion coefficient of early-age cement pastes were conducted followed by the separation of the thermal strain and the autogenous strain out of the total strain (hereafter we use 'autogenous strain' on behalf of 'autogenous shrinkage' because sometimes strain of cement paste or concrete due to self-desiccation by hydration shows expansion). During the measurement, specimens were subjected to high temperature histories imitating the hydration heat and to instantaneous thermal pulses to determine the thermal expansion coefficients at each age of the specimen.

Determination of the thermal expansion coefficient of early-age concrete, mortar or cement paste has been performed mostly by length change measurement during changes in temperature. The employed sensors included contact displacement gauge [6–8], laser displacement meter [9], vibrating wire extensiometer [10] and fiber-optic deformation sensor [11]. A dilatometer was also used when measurement begins immediately after mixing [12,13].

As Loser [13] pointed out, contact type gauges may not be appropriate if applied to specimens in a plastic state at very early stages because the contact pressure may pose some effects on the volume change of the specimen. The contact-free laser displacement meter may similarly be inappropriate when the specimen is not elastic enough to give changes in the gauge marks. However, as the existing studies have shown [6,7,9,10,12] that the thermal expansion coefficient decreases immediately after mixing and shows a minimum around the set point in accordance with the development of stiffness of the specimen, use of the reliable laser displacement meter to measure the post-setting thermal deformations may be allowed when

* Corresponding author. Tel.: +81 52 789 3761; fax: +81 52 789 3773.
E-mail address: ippei@dali.nuac.nagoya-u.ac.jp (I. Maruyama).

0008-8846/$ – see front matter © 2011 Elsevier Ltd. All rights reserved.
doi:10.1016/j.cemconres.2011.01.003

Table 1
Properties of Portland cement.

	Density (g/cm^3)	Blane value (cm^2/g)	Ig loss (%)	Chemical composition (%mass)								
				SiO_2	Al_2O_3	Fe_2O_3	CaO	MgO	SO_3	Na_2O	K_2O	Cl^-
N	3.16	3110	0.64	21.8	4.49	2.90	63.9	1.84	2.26	0.20	0.38	0.007

Table 2
Properties of Blast furnace slag.

	Density (g/cm^3)	Blane value (cm^2/g)	Ig loss (%)	Chemical composition (%mass)										
				SiO_2	Al_2O_3	FeO	CaO	MgO	S	Na_2O	K_2O	TiO_2	MnO	Cl
BB	2.90	4050	0.05	33.88	15.34	0.34	42.65	5.81	0.65	0.28	0.31	0.57	0.16	0.004

studying the crack mechanisms of mass concrete and stress-induced strains.

For a specimen with a large cross-section, on the other hand, temperature distribution in the specimen and resulting restrained stresses are likely to affect the measurement, hence a specimen as thin as possible and a thermostat apparatus with a large heat capacity are needed. In this aspect, use of the laser displacement meter is more advantageous in measuring thin specimens.

In this study, the thermal expansion coefficient was determined with a laser displacement meter using 10 mm thick specimens at ages immediately after setting where thermal expansion coefficient shows the minimum. This method is similar to the experiment by Ø. Bjøntegaard and E. J. Sellevold [6], but the thickness of the specimen and the displacement measurement are much carefully treated.

2. Outline of the experiments

2.1. Materials used and mixing procedure

Binder types used in this experiments were OPC, GGBFS and anhydrite with a specific surface area of 4690 cm^2/g. Properties of OPC and GGBFS are shown respectively in Tables 1 and 2, and the binder compounds were the OPC single use (denoted as N) and GGBFS substituted 3.4% with anhydrite, the latter further substituted for the OPC by 30% (denoted as BB30) and 45% (denoted as BB45).

Water to binder ratios were 0.40 and 0.55 as suffixed −40 and −55. All the materials were kept under a constant temperature of 20 °C for 24 h before mixing. Each 20 kg of the binder was introduced to the Omni mixer and mixed for 3 min followed by a scraping and mixing of another 3 min. Mixing was performed under a room temperature of 25 °C, and the batch was moved to the room whose temperature is controlled at 20 °C just after mixing. Considerable bleeding as shown in cement pastes with a high water to binder ratio was prevented by the successive mixing of every 30 min for 4 h (in the case of N) and 6 h (in the cases of BB40 and BB55) till the bleeding was no longer observed. All the acquired data have their points of origin at the time when water was added.

2.2. Determination of changes in length and thermal expansion coefficient

2.2.1. Specimens and test apparatus

The length change measuring apparatus used in the experiments is shown in Fig. 1. Dimensions of the specimen subjected to the length change measurement was 10×60×370 mm which was thin enough to ensure uniform temperature distribution within the specimen. The longitudinal direction of the specimen with a measuring distance of 300 mm was measured with two laser displacement meters at a resolution of 0.5 μm.

Specimen temperature was controlled by circulating the thermostatic water in the hollow copper mold around the specimen using a thermostatic bath (heating capacity of 1.0 kW, cooling capacity of 150 W and flow rate of 15 l/min) as shown in Fig. 2. The copper mold and the specimen were thermally insulated with a polystyrene foam of 30 mm thick to minimize heat exchange with the room air. Specimens were wrapped with a polyester film with a thickness of 0.05 mm to prevent friction between the cement paste and the copper plate and to prevent drying of the specimen.

The preliminary test has shown that the performance of the temperature control system regarding the temperature difference inside of a specimen was within ±0.2 °C both in longitudinal and horizontal directions, hence the representative specimen temperature was presumed as the averaged temperature of two thermocouples located at the center and the end of a specimen. In addition, the difference between imposed temperature and specimen's temperature is less than 0.4 °C.

At the age of 168 h, specimens were removed from the apparatus, and polyester film was stripped, then, two strain gauges (30 mm in measuring length) with a stainless steel foil base applied to the specimen and specimen was re-sealed with an aluminum adhesive tape with a thickness of 0.05 mm to avoid specimen drying, and placed

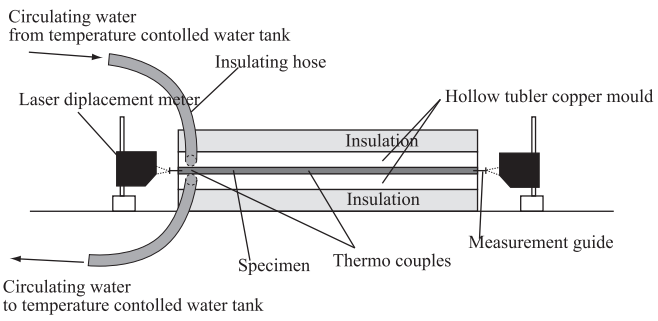

Fig. 1. Setup of displacement measuring system.

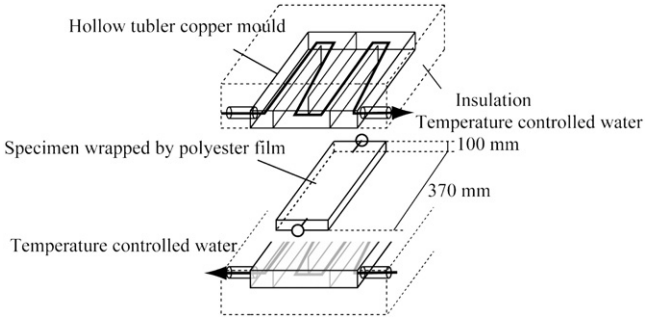

Fig. 2. Detail of copper mould.

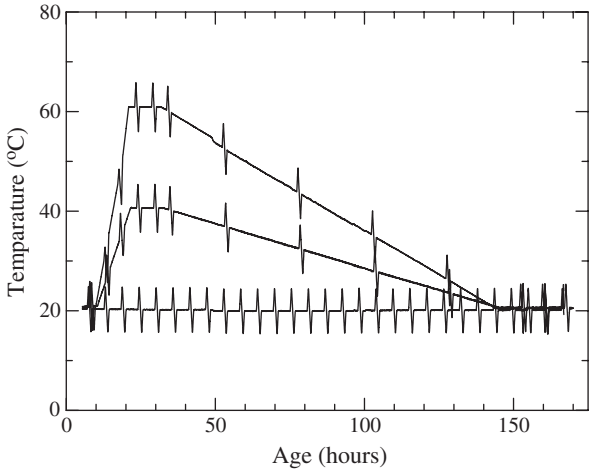

Fig. 3. Applied temperature histories.

in a thermostatic chamber at a temperature of 20 ± 2 °C. Measurement of autogenous strain after the age of 168 h was performed in this manner. As generally accepted in the continuum mechanics, deformation of specimens in this paper is denoted by positive for expansion and by negative for shrinkage.

2.2.2. Temperature histories and determination of total strain and thermal expansion coefficient

Three temperature histories were applied to the specimen namely 20 °C—constant (denoted as −20), elevated up to 60 °C (denoted as −60) and elevated up to 40 °C (denoted as −40). The latter two were meant to simulate the hydration heat-induced temperature history in concrete such that keeping 20 °C for the first 10 h and increasing up to the maximum temperature within 12 h with a temperature increasing rate of 3.33 °C/h (in the case of max. 60 °C) and 1.67 °C/h (in the case of max. 40 °C). After reaching the maximum temperatures, they are kept for 10 h and cooled at the age of 32 h to reach 20 °C at the age of 144 h. The temperature decreasing rates were 0.357 °C/h (in the case of max. 60 °C) and 0.179 °C/h (in the case of max. 40 °C).

Simultaneous with the above temperature histories, short thermal pulses were applied to the specimens to determine the thermal expansion coefficient at each material age. The thermal pulse was plus and minus 5 °C with a rate of 0.2 °C/min and applied every 340 min for the specimen kept under the constant temperature of 20 °C and, for the specimens subjected to maximum temperature of 60 and 40 °C, at ages of 7, 13, 18, 23, 28, 33, 52, 77, 102, 127, 152, 159, and 166 h as shown in Fig. 3.

A typical temperature change profile and associated thermal strains by a thermal pulse are shown in Fig. 4. For simplicity, the point of origin of strain was set to be zero when a thermal pulse is applied in this figure. As shown in Fig. 4, a thermal pulse comprises four steps: an increase for 5 °C (Step 1), a decrease for −5 °C (Step 2), further decrease for −5 °C (Step 3) and a recovery increase for +5 °C. Increasing and decreasing rates of temperature in a pulse were 0.2 °C/min. With a constant baseline, the applied temperature change will return to the baseline after a Step 2 decrease and/or a Step 4 increase.

Thermal expansion coefficient was estimated as an average of those at increase and decrease in temperature, which allowed canceling the autogeneous strain that was assumed to develop constantly during the period of a pulse. For a less data fluctuation, the first and the last 0.5 °C in the temperature change of a pulse were omitted and the other data with a higher linearity was subjected to the regression analysis. Also, the average of a convex pulse, Step 1 and Step 2, and that of a concave pulse, Step 3 and Step 4 are then averaged as the thermal expansion coefficient of the age was defined as the midpoint age of the four pulses.

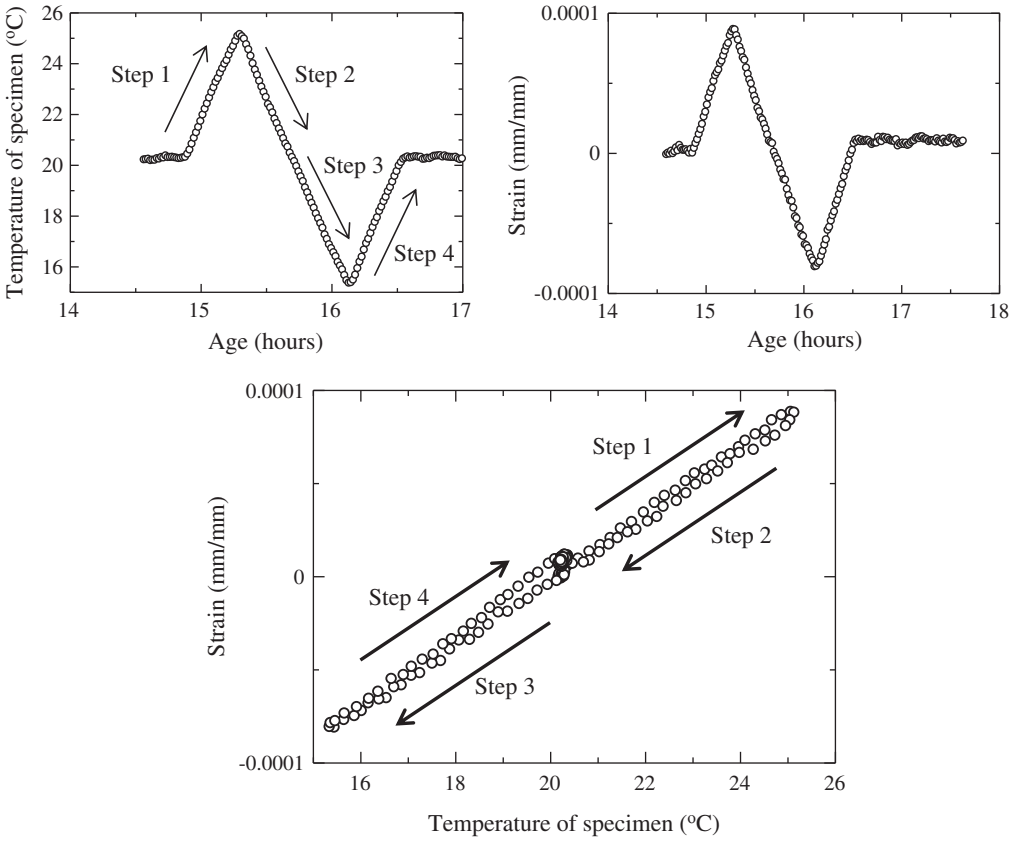

Fig. 4. Representative results of temperature and deformation strain during thermal pulse with constant base line.

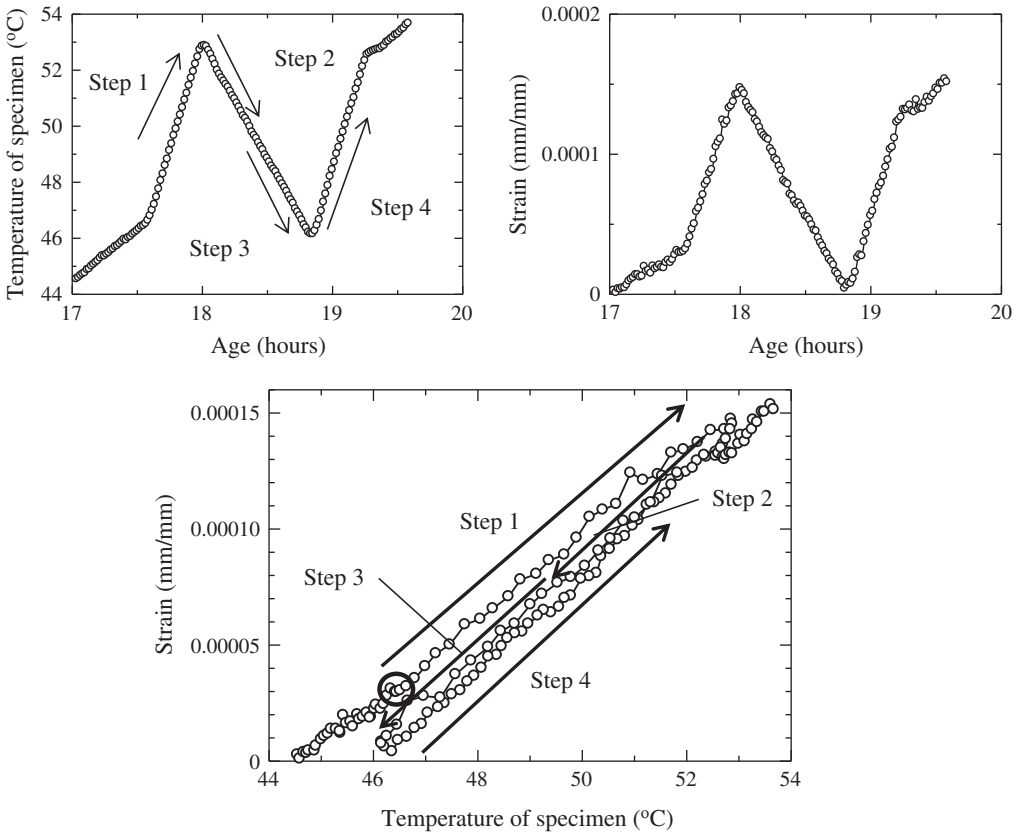

Fig. 5. Representative results of temperature and deformation strain during thermal pulse under increasing temperature base line.

A typical temperature-strain profile of N55–60 at the age closed to 18 h is shown in Fig. 5. When the baseline was either descending or ascending, an additional rate of 0.2 °C/min was added to the baseline. As a result, the time necessary for a step was not equal with that of the flat baseline. The preliminary test has shown that the influence of the thermal pulse on the total strain was negligible because it was within 5% at the age of 7 days [14]. The statistical error of this set-up is $\sigma = 1\ \mu/°C$.

2.2.3. Determination of autogenous strain

The points of origin for the volume change measurement were those at the age of 7.4 h and 6.7 h for W/B = 0.55 and 0.40 respectively. These values were determined by confirming the data acquisition from the specimens of N, BB0 and BB45.

Determination of autogenous strain was performed by subtracting the thermal strain from the total strain. The measured thermal

Table 3
Coefficient of Eqs. (1) and (2) for thermal expansion coefficient data of each cement paste.

	Max. temp.	t_0	a	b	c	d	e	f	g	h
N-40	20	56.4	40	0.27	0.1	19	5	40	0.01	6
	40	21.2					4.1	12	0.03	11
	60	17.3					5	10	0.07	11
N-55	20	104.3	60	0.3	−0.6	22	1	75	−0.02	16
	60	126.9	50	0.23	−1	20	0.6	120	0	14
BB30–40	20	105.0	70	0.30	1.0	14	5.2	85	−0.02	4
	40	42.7					4.7	24	0	4
	60	19.7					4.0	15	0.05	7
BB30–55	20	135.1	40	0.27	0.1	18	2	20	0.01	14
	60	30.3					3.5	115	0	8
BB45–40	20	68	50	0.23	1	14	3.8	30	−0.05	4
	40	35.3	50	0.23	1	17	3.5	30	−0.02	11
	60	22.3	50	0.23	1	14	4	15	0.04	13
BB45–55	20	117.9	40	0.18	0.1	18	3	85	0	8
	60	26.5					2.8	20	0.02	14

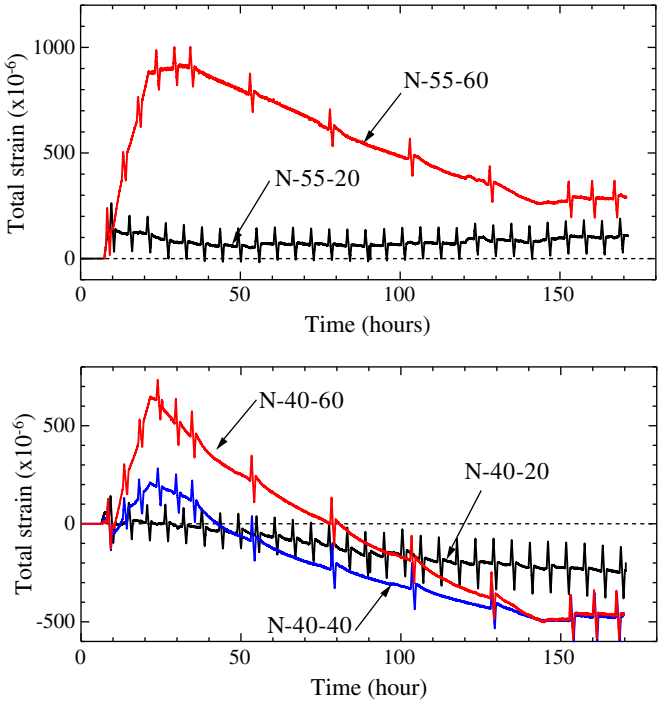

Fig. 6. Total deformation under controlled temperature history of hardened cement paste with water to cement ratio of 0.55 and 0.40 (N-55 and N-40).

expansion coefficient was subjected to curve fitting using Eqs. (1) and (2) followed by the calculation of incremental autogenous strain using Eq. (3).

$$\alpha(t) = a \cdot exp(b \cdot t) + c \cdot ln(t) + d, t < t_0 \quad (1)$$

$$\alpha(t) = e \cdot exp(t - f) + g \cdot t + h, t \geq t_0 \quad (2)$$

$$\Delta\varepsilon_{tot,i} = \Delta\varepsilon_{aut,i} + \frac{\alpha_i + \alpha_{i-1}}{2} \cdot (T_i - T_{i-1}) \quad (3)$$

where t: specimen age (hour), $\alpha(t)$: thermal expansion coefficient at the age t (10^{-6}), t_0: the specimen age when Eq. (1) assigns its applicability to Eq. (2), a to h: experimental constants, $\Delta\varepsilon_{tot,i}$, $\Delta\varepsilon_{aut,i}$: incremental total and autogenous strain at ith interval (10^{-6}), α_i: thermal expansion coefficient at ith interval (10^{-6}/°C), and T_i: specimen temperature at ith interval (°C). The unit interval was 1 h. For the determination of each coefficient, non-linear curve fitting was conducted.

Eqs. (1) and (2) are designed for curve-fitting purpose. Because the applied data were the thermal expansion coefficient averaged from a set of thermal pulses at respective temperatures, applicable range of the equations may be limited to the temperature range of a thermal pulse of ±5 °C. However, the calculation of autogeneous strain was based on the incremental strain every 1 h, hence the separation of strains may not be affected by the applicable range of the equations (Table 3).

3. Results

3.1. Total strain

Measured total strains of N-55 N-40, BB30–55, BB30–40, BB45–55, BB45–40 are shown in Figs. 6, 7 and 8. Strain of the specimens with W/B = 0.55 (N55 BB30–55 and BB45–55) at the age of 160 h, i.e. the end of the temperature history, were larger for those subjected to the temperature history than those without it. However, for specimens with W/B = 0.40, all the specimens subjected to the early-stage high temperature history showed larger residual shrinkage strain at the age of 160 h than that cured under the constant temperature of 20 °C. The shrinkage strains of specimens with the maximum temperature of 40 °C and 60 °C at the age of 160 h were equal for N40. For BB30, specimens subjected to a temperature history with the maximum temperature of 40 °C showed larger shrinkage strain than that of 60 °C while the result for BB45 was the reverse.

3.2. Thermal expansion coefficient

Thermal expansion coefficient calculated on the basis of the total strain data and the thermal strain at each pulse is shown in Figs. 9, 10 and 11. The error bars show the difference between the average of thermal expansion coefficients obtained with concave and convex thermal pulses. The upper values are taken over mostly with the convex pulse. It is shown that the thermal expansion coefficient of N-55 does not change significantly over the period from10–20 h to 160 h, while that of N-40 increases with time. The age when the increase in thermal expansion coefficient begins becomes earlier with an increase in the given maximum temperatures. This trend is implying an effect of cement hydration. Sellevold and Bjøntegaad have confirmed the time-dependant increase in thermal expansion coefficient in the experiment and pointed out it is attributed to the self-desiccation [15]. Their experiments also took into account the temperature history imitating the hydration heat and the early-stage increase in thermal expansion coefficient depending on the maximum temperature was also confirmed.

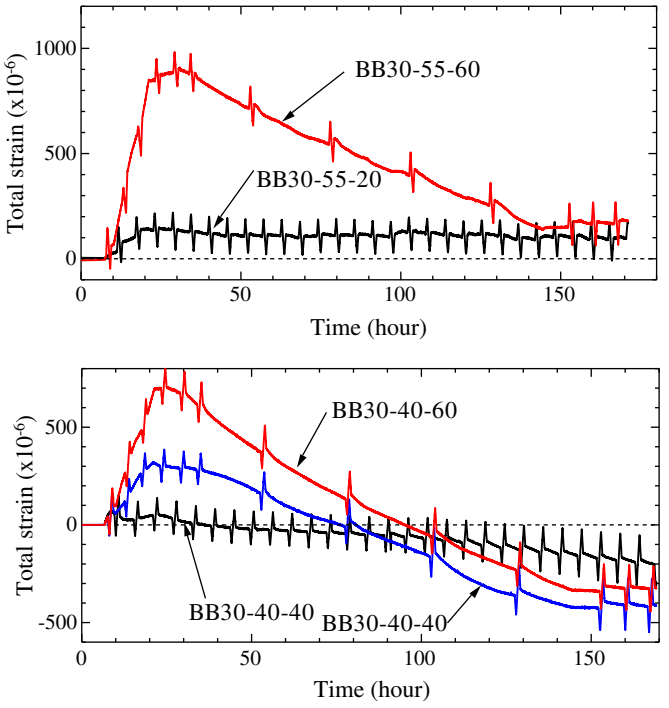

Fig. 7. Total deformation under controlled temperature history of hardened cement paste in which 30%-cement is replaced with granulated blast furnace slag with water to cement ratio of 0.55 and 0.40 (BB30–55, BB30–40).

When GGBFS was added, the increase in thermal expansion coefficient started at the age of 130 h for specimens with W/B = 0.55 under the constant temperature of 20 °C. This tendency reproduced when temperature histories imitating hydration heat were applied and the amount of increase was larger in BB45 than in BB30.

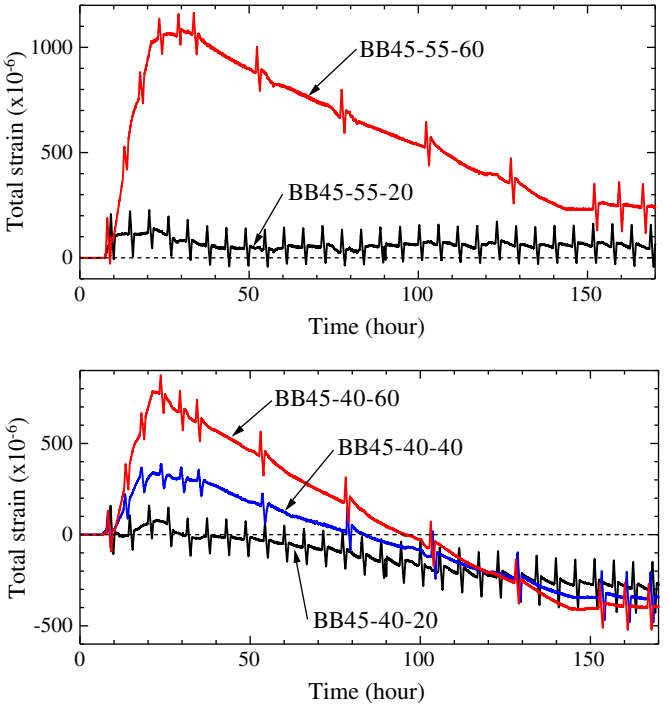

Fig. 8. Total deformation under controlled temperature history of hardened cement paste in which 45%-cement is replaced with granulated blast furnace slag with water to cement ratio of 0.55 and 0.40 (BB45–55, BB45–40).

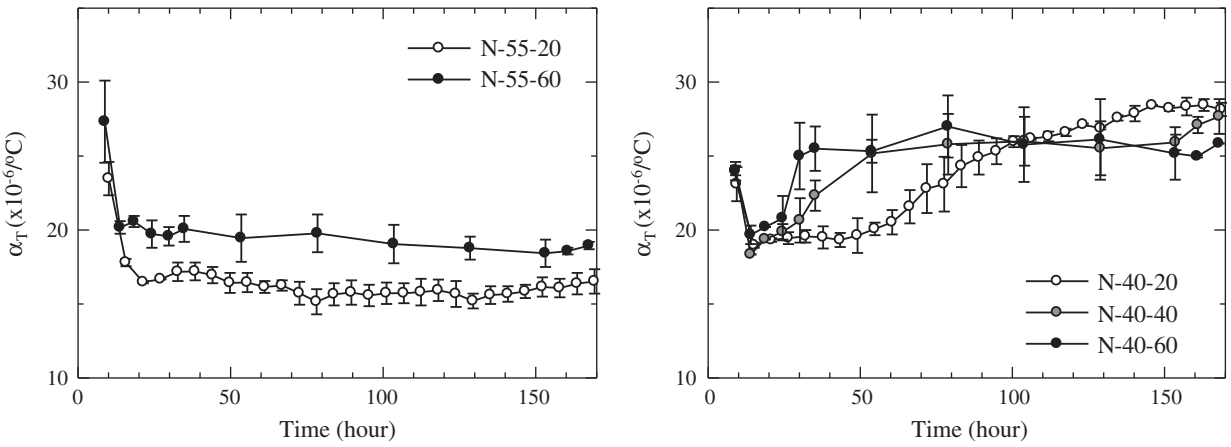

Fig. 9. Time-dependent thermal expansion coefficient (α_T) of N-55 and N-40.

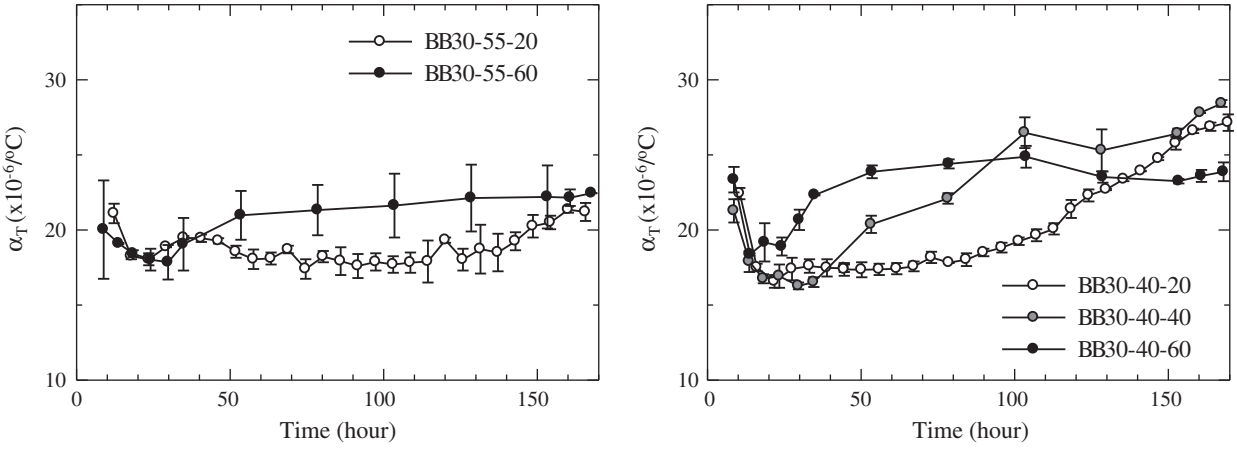

Fig. 10. Time-dependent thermal expansion coefficient (α_T) of BB30–55 and BB30–40.

This may be attributed to the early-stage self-desiccation compared to N due probably to the formation of high water content hydration products [16] such as C_4AH_{13}, C_3AH_6 and monosulfate, and the formation of C–S–H of low C/S molar ratio which adsorbs much water on its surface.

3.3. Separation of autogeneous strain from the total strain

The thermal strain and the autogenous strain of the cement paste were separated using the measured total strain and thermal expansion coefficient. This procedure is based on a commonly

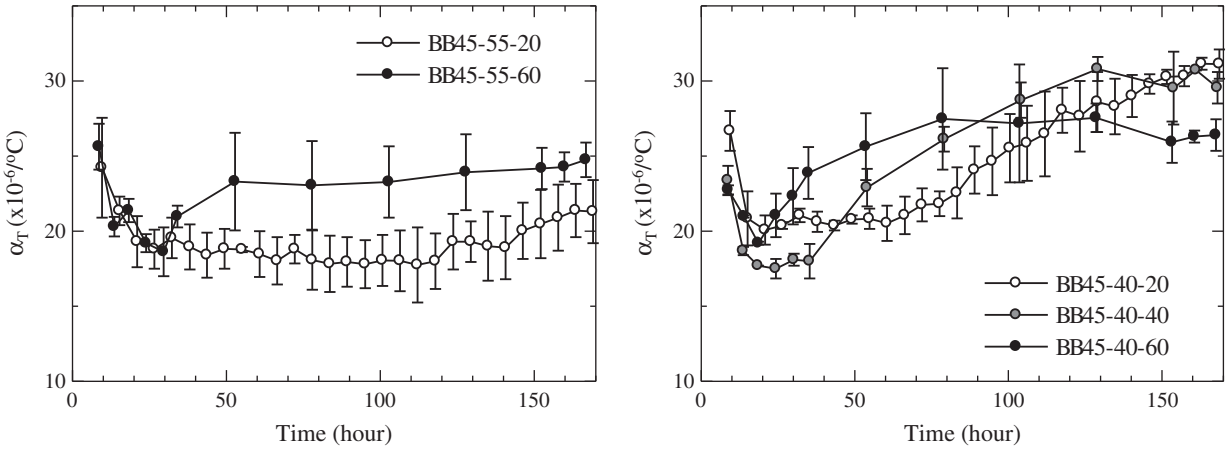

Fig. 11. Time-dependent thermal expansion coefficient (α_T) of BB45–55 and BB45–40.

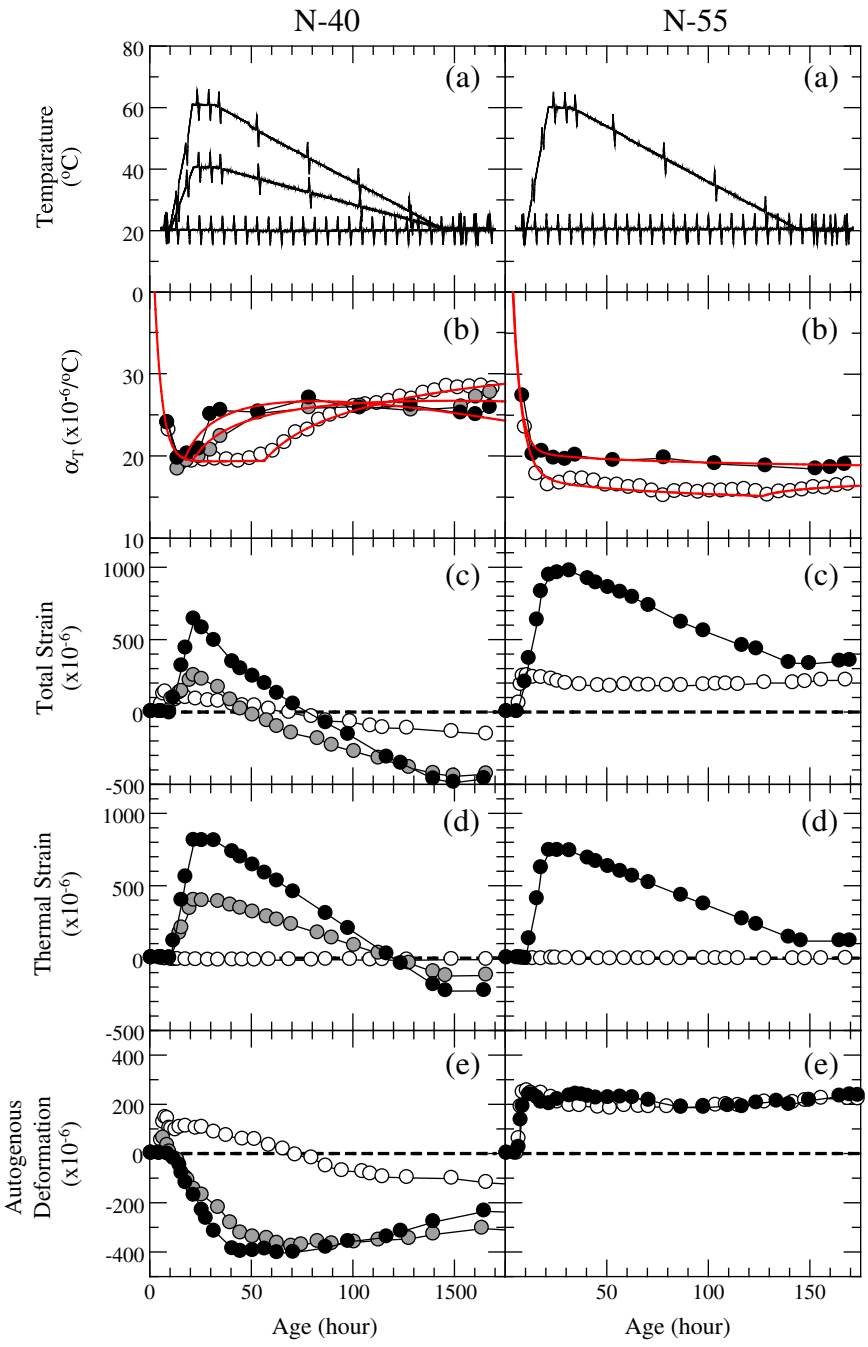

Fig. 12. Temperature history, thermal expansion coefficient, total strain, thermal strain and autogenous shrinkage of N55 and N40.

accepted engineering concept that the factors affecting volume change can be additive. The results are shown in Figs. 12 to 14.

3.3.1. Thermal strain and thermal expansion coefficient

Thermal expansion coefficient as a function of time was determined by curve fitting using Eqs. (1) and (2) as shown in Section 2.2.3. The results of the curve fitting are shown in the solid lines together with the experimental data of thermal expansion coefficient in Figs. 12 to 14.

The time-dependant thermal expansion coefficient, as described in Section 3.2, poses considerable impact on thermal strain because the difference in the thermal expansion coefficient between temperature increase process and decrease process results in a shrinkage strain. This mechanism could independently become a cause of thermal crack in mass concrete constructions.

When W/B is relatively high such as in N-55, the thermal expansion coefficient was nearly unchanged even subjected to the temperature history with the maximum temperature of 60 °C. Hence, resulting from the large thermal expansion coefficient at a very early-stage, the thermal strain at the age of 7 days was on the expansion side as shown in Fig. 12(d) right.

When W/B is relatively low such as in N-40, the thermal expansion coefficient showed a minimum nearly at the age of one day and increased subsequently. Hence the thermal strain at the age of 7 days was on the shrinkage side, i.e. the thermal expansion coefficient under temperature ascending span is smaller than under temperature descending span it resulted in the shrinkage in the final stage as shown in Fig. 12(d) left.

A tensile stress originated from the restrained thermal strain due to the time-dependant increase in thermal expansion coefficient is, in

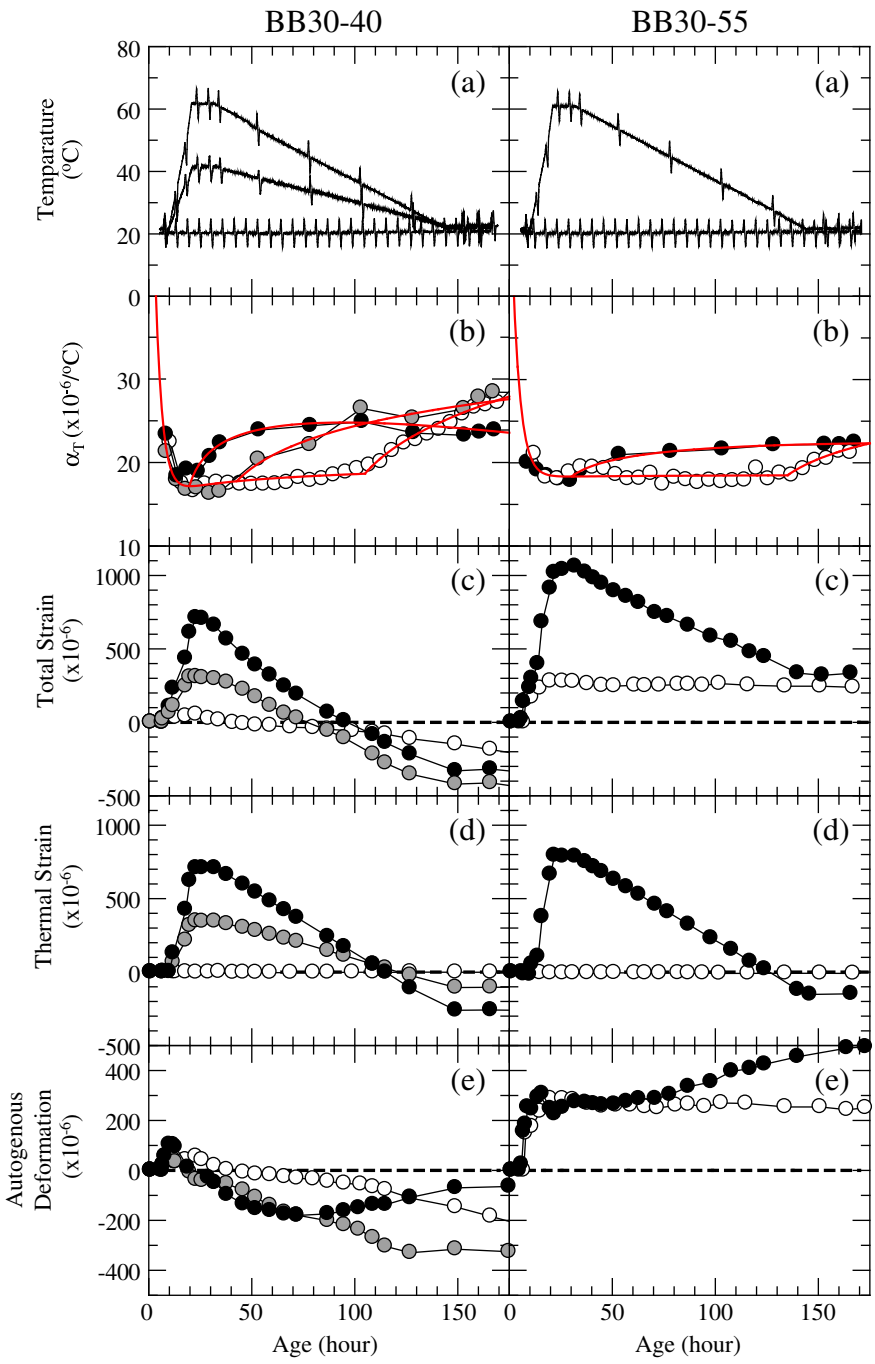

Fig. 13. Temperature history, thermal expansion coefficient, total strain, thermal strain and autogenous shrinkage of BB30–55 and BB30–40.

summary, the third factor affecting the thermal cracks of concrete subjected to the hydration heat-induced high temperature histories, among other factors including those due to the time-dependant change in Young's modulus of elasticity and autogenous shrinkage under external restraints.

Results of the type N, BB30 and BB45 are examined in this aspect. For the specimens with a W/B of 0.55, the thermal expansion coefficient of N-55 was unchanged even subjected to the temperature history with the maximum temperature of 60 °C, while that of BB30 and BB45 begun to increase at the age of 25 h. This implies the occurrence of early-stage self-desiccation in the presence of GBFS. This tendency corresponds to the changes with time of the thermal strains particularly the occurrence of shrinkage at the age of 7 days.

The strain change after reaching the maximum temperature is particularly important in mass concrete, and those were 638 μ for N-55, 711 μ for BB30–55 and 852 μ for BB45–55. These amounts of volume change are associated with the tensile stress under restrained conditions and correspond to the fact that the mass concrete with GGBFS is likely to form cracks.

For specimens with a W/B of 0.40, changes in thermal expansion coefficient of N-40, BB30–40 and BB45–40 and associated thermal strains showed no particular differences.

When the design of concrete structures is considered, mix design needs to be reexamined in terms of the design strength. Because water to binder ratio of blast furnace slag cement concrete tends to be lower than that of normal concrete for strength control reasons, and

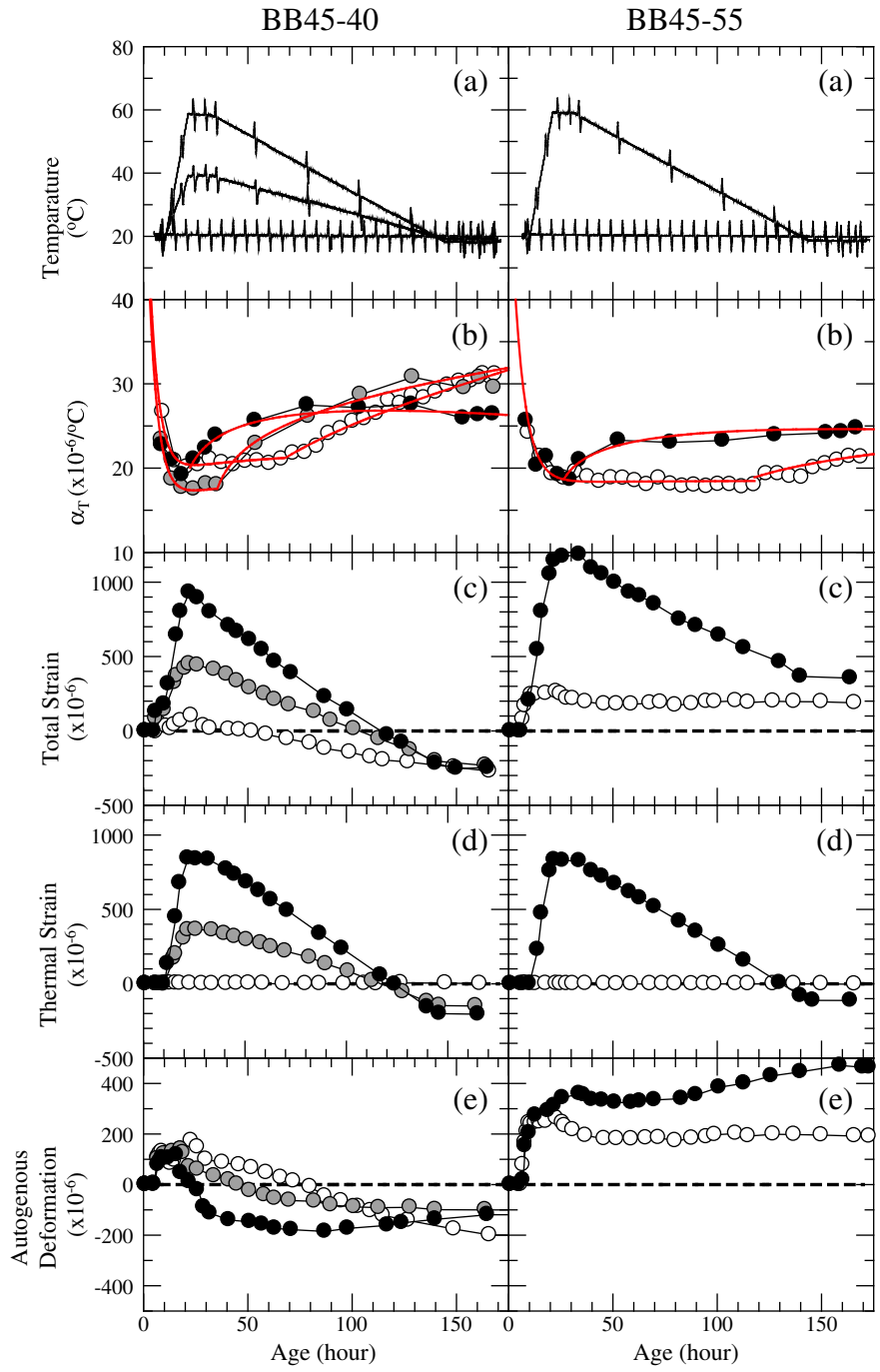

Fig. 14. Temperature history, thermal expansion coefficient, total strain, thermal strain and autogenous shrinkage of BB45–55 and BB45–40.

the density of GGBFS is smaller than that of cement, the mix proportion may result in a smaller aggregate content. In such a case, rigid comparison of thermal expansion coefficient between normal and blast furnace slag cement concrete is not easy because of the difference in their aggregate contents, but the effect of the thermal expansion coefficient seems to be still significant because smaller aggregate content increases the thermal expansion coefficient.

3.3.2. Autogenous strain

Autogenous strains of N-55 with maximum temperatures of 60 °C and 20 °C showed no particular difference and always in the expansion side, probably because N-55 had enough available water not to cause autogenous shrinkage. The expansion observed before the age of 24 h may be attributed to several reasons such as a mechanical effect due to ettringite formation [17] and an osmotic pressure acting on the liquid bridge between particles to disjoin each other, but the mechanisms still needs to be investigated. A pioneering research on the autogenous shrinkage by Tazawa and coworkers [2] showed such expansion more than 200 μ even under a constant temperature of 20 °C.

The absence of the difference between autogenous strain of N-55–60 and N-55–20 may be partly attributed to the large water to binder ratio enough to prevent the self-desiccation.

On the other hand, the autogenous strain of N-40 series are apparent and, at the age of 7 days, N-40–60 and N-40–40 showed particularly larger values than that cured under the constant temperature of 20 °C. A noteworthy time-dependent behavior was the autogenous shrinkage developing rapidly before reaching the maximum temperature in contrast to the subsequent slow and expansive development. This was

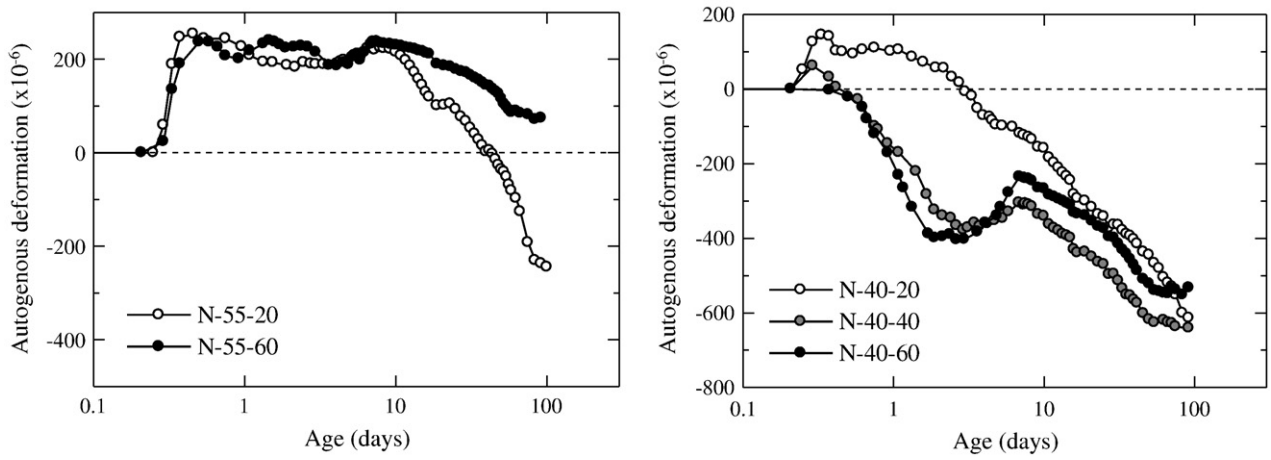

Fig. 15. Autogenous shrinkage of N-55 and N-40.

commonly found in specimens BB30 and BB45 subjected to the temperature histories.

For specimens with a W/B of 0.55 and with GGBFS, autogenous strain developed always on the expansion side and showed further expansion for those subjected to the temperature history with a maximum temperature of 60 °C as shown in Figs. 13(e) and 14(e) right. The total strain of BB45–55 subjected to the maximum temperature of 60 °C also showed expansion at the end of the temperature history compared to that cured under 20 °C. This behavior needs further investigation into the chemical composition of GGBFS, gypsum content and the timing to give a temperature history.

The turnaround of the autogenous strain from shrinkage to expansion trend after reaching the maximum temperature is a definite behavior commonly found in all the specimen type except for N-55. The same phenomenon was also found in the concrete specimens subjected to an imitated hydration heat and the turnaround from shrinkage to expansion after the temperature history was reported [18] while more investigation is needed to discuss with the behavior in terms of the volume change mechanisms.

The maximum autogenous strain of BB30–40 at the age of 7 days was observed when subjected to the maximum temperature of 40 °C. A close look at the thermal expansion coefficient shows it was the specimens subjected to the maximum temperature of 40 °C that the largest thermal expansion coefficient was recorded. This implies the difference in hydration products and properties of hardened cement paste according to the path of the temperature history.

The measurement of volume changes prolonged using the strain gauge are shown in Figs. 15, 16 and 17. Specimens subjected to the temperature histories showed a turnaround from expansion trend to shrinkage trend after the age of 7 days, and the shrinkage behavior exhibited similar tendency with those kept under the constant temperature of 20 °C. The post 7-day shrinkage of specimen without GGBFS and the temperature history was greater than that with the temperature history, while those with GGBPS showed almost similar shrinkage behavior.

4. Discussions

When the strain of cement paste subjected a temperature history at early ages was separated into thermal strain and autogenous strain without assuming that the thermal expansion coefficient be constant throughout, a new phase of the volume change problem emerged. Namely, a larger average thermal expansion coefficient during temperature decreasing period than that during temperature increasing period poses an additional shrinkage strain after the temperature history. Because the increase in the thermal expansion coefficient is originated from the consumption of water with hydration, i.e. self-desiccation, the impact could be more significant when the mix proportion and materials favorable to self-desiccation are employed.

The proportion of the thermal strain, i.e. the thermal contraction due to the time-dependent increase in thermal expansion coefficient, in the total strain at the age of 7 days after the temperature history with the maximum temperature of 60 °C is shown in Fig. 18. The

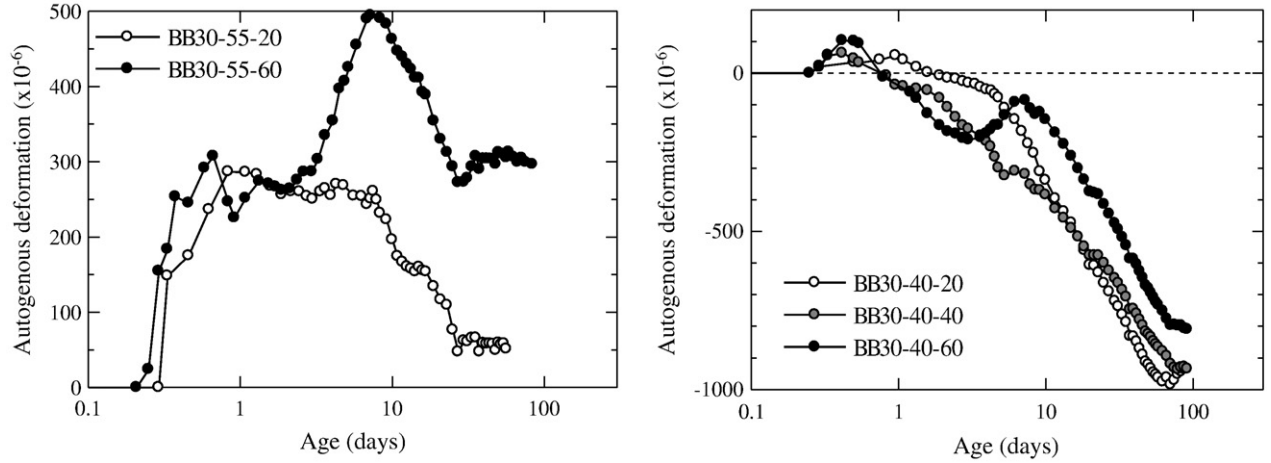

Fig. 16. Autogenous shrinkage of BB30–55 and BB30–40.

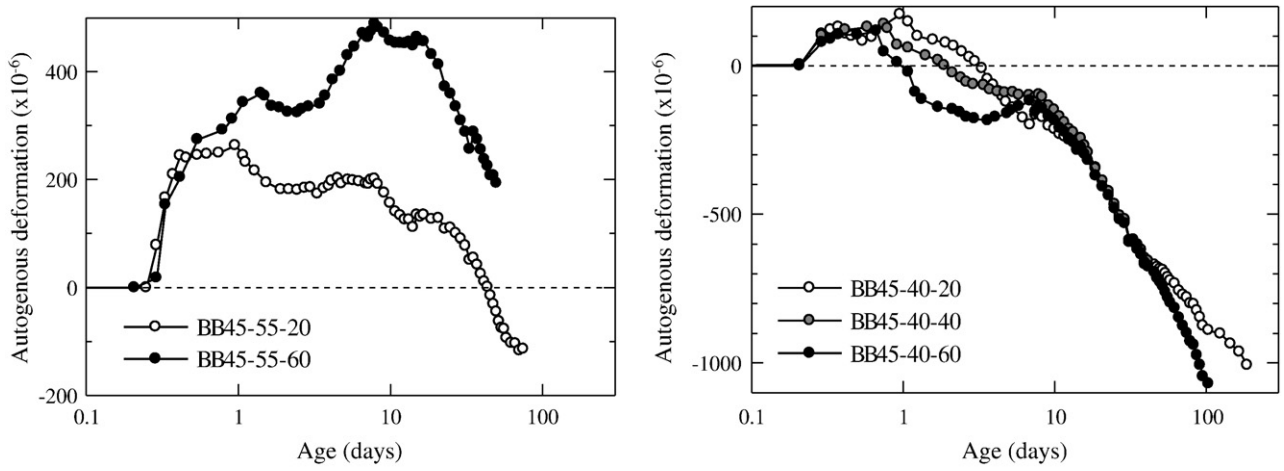

Fig. 17. Autogenous shrinkage of BB45–55 and BB45–40.

fraction of the thermal strain extends over 80% for specimens with a W/B of 0.40 and with GBFS, and for specimens with a W/B of 0.55 and with GBFS, thermal strain was still contraction in contrast to the total strain of expansion.

The volume change due to the time-dependant thermal expansion coefficient and increasing and decreasing temperature history may be a component of autogenous shrinkage, because it is a result of interaction between self-desiccation and the temperature history. The additional contraction due to the temperature history highly correlates with the extent of the temperature increase. If the thermal expansion coefficient is constant during each increasing and decreasing process, the final amount of contraction depends on the maximum temperature. Hence it is a reasonable manner to evaluate the final autogenous shrinkage as a function of the maximum temperature when using a design formula taking account of the effect of temperature history due to hydration.

When the thermal cracking risk is evaluated by estimating the final total strain, use of a constant thermal expansion coefficient to separate the thermal strain and the autogenous shrinkage strain may be of significance in an engineering aspect. However, taking account of the findings of this study, any discussions on the autogenous shrinkage and cracking mechanisms or on the practical problems on the basis of the constant thermal expansion coefficient may lead to an oversight of the essence of the volume change behavior. The thermal expansion coefficient of concrete may behave differently due to the effect of aggregate but the overall mechanism will be carried out.

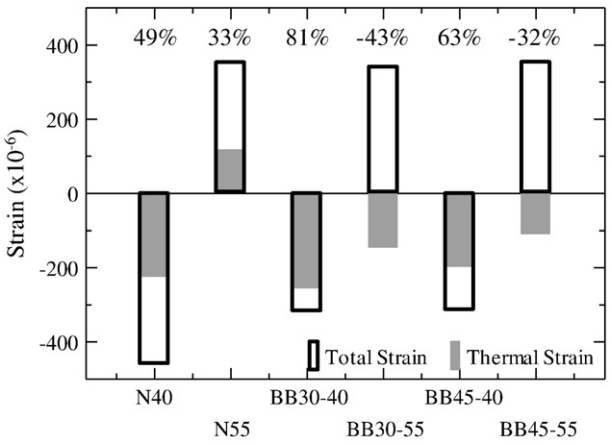

Fig. 18. Relationship between total strain and thermal strain due to time-dependent thermal expansion coefficient of each cement paste.

Discussion of the effect of expansive agent on the thermal cracking is a good example to demonstrate the finding of this study. The expansive reactions of the commercially available expansive agents of lime type or ettringite type may come to the end within 3 days under a room temperature [19] and even at earlier stage under adiabatic conditions. The expansion, when considered as a crack control of mass concrete, contributes to reduce the cracking risks generating a compressive stress under retrained conditions. However, the expansive reactions may result in rising the maximum temperature and excessive water consumption due to formation of calcium hydroxide and calcium aluminate hydrates, leading to the promotion of the self-desiccation and to increase of thermal expansion coefficient. This may exceed the compressive stress resulted from the use of expansive agent. At the ages when the compressive stress is accumulated, the concrete may exhibit a low Young's modulus of elasticity and a high creep coefficient, hence the setoff of this margin is very likely to occur. Under the assumption that the thermal expansion coefficient is unchanged throughout, the above discussion from the materials aspect cannot be possible hence the factors-separation approach is effective in estimating the materials' performance.

Prevention of the self-desiccation and resulting time-dependant increase in thermal expansion coefficient using water-releasing lightweight aggregate will be dealt with in the forthcoming paper emphasizing that the time-dependant increase in the thermal expansion coefficient due to self-desiccation plays an important role in the crack risk control.

Interactions with the reinforcing steel need to be considered for design. The conventional crack risk criteria assumed that the thermal expansion coefficients of steel and concrete are very close and the difference was often neglected in the analysis. However, as this study has shown, the stress redistribution may occur between steel and concrete when the thermal expansion coefficient changes with the development of hydration, especially after the occurrence of the maximum temperature. The stress redistribution may be mostly influenced by the thermal strains at the temperature decrease in addition to the development of bond and Young's modulus of concrete. Taking into account the stress release after cracking, the compressive stress accumulated in the steel reinforcement may result in widening of the crack width, which needs to be confirmed for the crack control of structural members. Regarding the difference in the thermal expansion coefficient, use of aggregate with a low thermal expansion coefficient such as limestone tends to be affected by the effect of temperature history due to hydration heat. The interface between cement paste and aggregates is most likely to be damaged

due to the difference in the thermal expansion coefficient implying the possible problems related to strength and durability.

5. Conclusions

In this study, volume changes and time-dependent increase in thermal expansion coefficient were determined at early stages and the measured total strain was separated into the thermal strain and the autogenous strain. Cement paste specimen with a water to binder ratio of 0.55 and 0.40 were partially replaced with ground granulated blast furnace slag for 30 and 45% and subjected to temperature histories that imitated hydration-induced temperature rise of the early-stage mass concrete. It was shown that the thermal expansion coefficient increased significantly with the development of hydration and became more conspicuous when the ground granulated blast furnace slag was added. The time-dependant increase of thermal expansion coefficient, due probably to self-desiccation, could result in considerable residual shrinkage strain at the end of the temperature history and promote the thermal cracks. The impact of the time-dependant increase of thermal expansion coefficient might be taken into account as one of the necessary factors in the crack control design from now and, within the range of the water to binder ratio of this study, cannot even be neglected and sometimes exceed the autogenous shrinkage.

References

[1] Y. Yang, R. Sato, T. Takeuchi, Study on thermal expansion coefficient of cement paste at early ages, Cem. Sci. Conc. Technol. 54 (2000) 209–214.
[2] E. Tazawa, S. Miyazawa, Influence of cement and admixture on autogenous shrinkage of cement paste, Cem. Conc. Res. 25 (1995) 281–287.
[3] Japan Concrete Institute, Guidelines for control of cracking of mass concrete 2008, Houkou-sha, , 2008.
[4] G. De Shutter, Finite element simulation of thermal cracking in massive hardening concrete elements using degree of hydration based material laws, Comput. Struct. 80 (2002) 2035–2042.
[5] Architectural Institute Japan, Recommendations for practice of thermal cracking control of massive concrete in buildings, 2008.
[6] Ø. Bjøntegaard, E.J. Sellevold, Interaction between thermal dilation and autogenous deformation in high performance concrete, Mater. Struct. 34 (2001) 266–272.
[7] M. Sarkis, J.L. Granju, M. Arnaud, G. Escadeillas, Coefficient de dilation thermique d'un mortier frais, Mater. Struct. 35 (2002) 415–420.
[8] Y. Yang, R. Sato, A new approach for evaluation of autogenous shrinkage of high strength concrete under heat of hydration, in: B. Persson, G. Fagerland (Eds.), Self-desiccation and its importance in concrete technology, 14–15 June 2002 (Lund Sweden), 2002, pp. 51–65.
[9] M. Ozawa, H. Morimoto, Estimation method for thermal expansion coefficient of concrete at early ages, in: Lura, Jensen, Kovler (Eds.), RILEM Int. Conf. Volume Changes of Hardening Concrete, 20-23 August 2006 (Lyngby, Denmark), 2006, pp. 331–339.
[10] H. Kada, M. Lachemi, N. Petrov, O. Bonneau, P.-C. Aitcin, Determination of the coefficient of thermal expansion of high performance concrete from initial setting, Mater. Struct. 35 (2002) 35–41.
[11] M. Viviani, B. Glisic, I.F.C. Smith, Separation of thermal and autogenous deformation at varying temperature using optical fiber sensors, Cem. Conc. Comp. 29 (2007) 435–447.
[12] A. Loukili, A. Chopin, A. Khelidj, J.-Y. Le Touzo, A new approach to determine autogenous shrinkage of mortar at an early age considering temperature history, Cem. Concr. Res. 30 (2000) 915–922.
[13] R. Loser, B. Münch, P. Lura, A volumetric technique for measuring the coefficient of thermal expansion of hardening cement paste and mortar, Cem. Conc. Res. 40 (2010) 1138–1147.
[14] A. Teramoto, I. Maryama, Study on temperature dependency of autogenous shrinkage of silica fume concrete with low W/B ratio, J. Struct. Constr. Eng. Trans. AIJ 73 (2008) 2069–2076, (in Japanese).
[15] E.J. Sellevold, Ø. Bjøntegaad, Coefficient of thermal expansion of cement paste and concrete: mechanisms of moisture interaction, Mater. Struct. 39 (2006) 809–815.
[16] W. Chen, H.J.H. Brouwers, The hydration of slag, part 1, 2, and 3, J. Mater. Sci. 42 (2007), 428-443, 444-464 and 9595-9610.
[17] I. Odler, J. Colán-Subauste, Investigations on cement expansion associated with ettringite formation, Cem. Concr. Res. 29 (1999) 731–735.
[18] H. Hashida, N. Yamazaki, Deformation composed of autogenous shrinkage and thermal expansion due to hydration of high-strength concrete and stress in reinforced structures, in: B. Persson, G. Fagerlund (Eds.), Proc. of self-desiccation and its importance in concrete technology, June 14–15, 2002, pp. 77–92, Lund Institute of Technology, Lund, Sweden.
[19] H. Ito, I. Maruyama, M. Tanimura, R. Sato, Early age deformation and resultant induced stress in expansive high strength concrete, J. Adv. Concr. Technol. 2 (2004) 155–174.